Neurochemistry International 146 (2021) 105032

Contents lists available at ScienceDirect

Neurochemistry International

journal homepage: www.elsevier.com/locate/neuint

LAMP2 deficiency attenuates the neurodegeneration markers induced by HSV-1 infection

Henrike Kristen [a,b], Isabel Sastre [a,b], Sara Aljama [a], Maria Fuentes [a], Maria Recuero [a,b,c], Ana Frank-García [b,c], Angel Martin [b,c], Pascual Sanchez-Juan [b,d], Carmen Lage [b,d], Maria J. Bullido [a,b,c,**], Jesus Aldudo [a,b,c,*]

[a] Centro de Biologia Molecular "Severo Ochoa" (C.S.I.C.-U.A.M.), Universidad Autonoma de Madrid, Madrid, Spain
[b] Centro de Investigacion Biomedica en Red sobre Enfermedades Neurodegenerativas (CIBERNED), Madrid, Spain
[c] Instituto de Investigación Sanitaria del Hospital Universitario La Paz – IdiPAZ (Hospital Universitario La Paz – Universidad Autónoma de Madrid), Madrid, Spain
[d] Hospital Universitario Marqués de Valdecilla-IDIVAL-UC, Santander, Spain

ARTICLE INFO

Keywords:
LAMP2
HSV-1 infection
Herpesvirus
Lysosome
Neurodegeneration
Alzheimer's disease
Genetic association

ABSTRACT

Mounting evidence suggests a major role of infectious agents in the pathogenesis of sporadic Alzheimer's disease (AD). Among them, herpes simplex virus type 1 (HSV-1) infection has emerged as a major factor in the etiology of AD. HSV-1 is able to induce some of the main alterations of the disease such as hyperphosphorylation of tau protein and accumulation of amyloid-β peptide. Functional genomic analysis of a cell model of HSV-1 infection and oxidative stress developed in our laboratory revealed lysosomal system to be the main pathway altered, and the lysosome-associated membrane protein 2 (*LAMP2*) gene one of the most strongly modulated genes. The aim of this work is to study *LAMP2* as an AD candidate gene and to investigate its role in the neurodegeneration induced by HSV-1 using a LAMP2 knockdown cell model. LAMP2 deficiency led to a significant reduction of viral DNA replication and formation of infectious particles. In addition, tau hyperphosphorylation and inhibition of Aβ secretion induced by the virus were attenuated by the absence of LAMP2. Finally, genetic association studies revealed LAMP2 genetic variants to be associated with AD risk. In summary, our data indicate that LAMP2 could be a suitable candidate to mediate the AD-like phenotype caused by HSV-1.

1. Introduction

The understanding of the pathogenic mechanisms of Alzheimer's disease (AD) remains a formidable challenge for the scientific community, and is needed for the development of better diagnostic methods and therapeutic interventions. A growing body of evidence supports the participation of chronic or latent infections of the central nervous system in the neurodegenerative process, by a direct effect of the infectious agent and/or by the associated inflammatory responses (Ashraf et al., 2019). Among them, herpesvirus infections induce similar hallmark features to those observed in AD brains and, particularly, HSV-1 has been suggested to play a role in AD development (Marcocci et al., 2020; Qin and Li, 2019). Numerous findings point to the active involvement of HSV-1 infection in AD pathogenesis. Epidemiological studies showed that people infected with HSV-1 who also carried the apolipoprotein E type 4 allele were at higher risk of developing the disease (Itzhaki et al., 1997). Moreover, HSV-1 DNA is present in the brains, mainly within amyloid plaques, of a high proportion of people with AD (Wozniak et al., 2009). Analysis of data gathered in genome-wide association studies involving thousands of AD patients and controls identified a set of AD-linked gene variants that might increase brain susceptibility to viral infections, particularly HSV-1 infection (Lambert et al., 2009; Porcellini et al., 2010). The presence of anti-HSV-1 IgM antibodies in serum, a sign of HSV-1 reactivation, was also correlated with an increased risk of developing AD (Letenneur et al., 2008; Lovheim et al., 2015, 2019).

Recently, three reports have provided strong evidence of the involvement of HSV-1 in the pathogenesis of AD. Multiscale analysis integrating genomic, transcriptomic, proteomic, and histopathological data provided compelling evidence that several herpesviruses (HSV-1; HHV-6A and HHV-7) contribute to the development of neuropathology

* Corresponding author. Centro de Biología Molecular "Severo Ochoa", Universidad Autónoma de Madrid, C/ Nicolás Cabrera 1, 28049, Madrid, Spain.
** Corresponding author. Centro de Biología Molecular "Severo Ochoa", Universidad Autónoma de Madrid, C/ Nicolás Cabrera 1, 28049, Madrid, Spain.
E-mail addresses: mjbullido@cbm.csic.es (M.J. Bullido), jaldudo@cbm.csic.es (J. Aldudo).

https://doi.org/10.1016/j.neuint.2021.105032
Received 8 October 2020; Received in revised form 18 March 2021; Accepted 22 March 2021
Available online 27 March 2021

and AD (Readhead et al., 2018). A second study showed a significant risk reduction of developing dementia in patients affected by HSV infections upon treatment with anti-herpetic medications (Tzeng et al., 2018). Finally, a study performed in mice and in 3D cultures of human neurons demonstrated that amyloid-β (Aβ) oligomers are able to bind herpesvirus surface glycoproteins, thus accelerating Aβ deposition and leading to protective viral entrapment activity (Eimer et al., 2018). The participation of HSV-1 in AD is further supported by the discovery that murine models of HSV-1 infection display similar changes to AD pathology (Li Puma et al., 2019; Protto et al., 2020). Recent advances in human stem cell and three-dimensional (3D) culture technologies have made possible the generation of novel 3D neural cell culture models that recapitulate AD pathogenic cascades, including Aβ and phospho-tau pathologies (Cenini et al., 2020). In that way, HSV-1-infection 3D cell models have been reported to partially mimic the characteristic pathology of the disease (Abrahamson et al., 2020; Cairns et al., 2020; D'Aiuto et al., 2019; Qiao et al., 2020). These models constitute an excellent study platform to elucidate mechanisms of HSV-1-mediated AD pathogenesis and to identify potential targets for treating this disease.

Our group has devoted several years to the development and study of neuronal models that simulate different aspects of AD pathogenesis, such as HSV-1 infection and oxidative stress. With this strategy, we have shown that HSV-1 is able to trigger the neurodegenerative process inducing the appearance of the characteristic markers of AD-type neurodegeneration (Alvarez et al., 2012; Santana et al., 2012a). Functional genomic analysis of the infected cells, specially when the infection is induced in the presence of a mild oxidative stress mimicking that present in aged brains, revealed that the main pathway altered was the lysosomal system, and the *LAMP2* gene was one of the most strongly modulated (Kristen et al., 2018).

Lysosomes are acidic, membrane-bound organelles containing proteases, lipases and nucleases and are involved in turnover of cargoes from autophagic and endocytic pathways to regenerate catabolic precursors for cellular use (Settembre et al., 2013). Neurons especially rely on functional lysosomal degradation since they live extremely long without cell division. It is therefore not surprising that defects in autophagy and endocytosis are relevant to neurodegenerative diseases, in particular to AD. Indeed, substantial links between AD pathogenesis and lysosomal biology have been reported (Nixon, 2017; Whyte et al., 2017). Endocytosis impairment, enlargement of endosomal compartments, progressive accumulation of autophagic vesicles, altered trafficking of lysosomal enzymes, and deficits of lysosomal function are all well recognized as early neuropathological features of sporadic AD (Peric and Annaert, 2015). Accordingly, recent results of our group showed a series of HSV-1-induced anomalies in the functional status of lysosomal pathway provoking a strong decrease in lysosomal degradative activity (Kristen et al., 2018). Together, these findings support the hypothesis that alterations in lysosomal function might contribute significantly to the neurodegeneration associated with AD and HSV-1 infection.

The limiting membrane of lysosomes is lined with the lysosomal associated membrane glycoproteins (LAMPs). LAMP1 and LAMP2 constitute about half of all proteins of the lysosomal membrane, but little is known about their function. LAMPs are comprised of a short cytoplasmic domain, a single transmembrane span, and a highly N- and O-glycosylated luminal domain (Eskelinen et al., 2003). Because of their abundance and glycan content, LAMPs have been proposed to serve as a protective barrier to block hydrolase access to the lysosomal membrane (Kundra and Kornfeld, 1999). LAMP2 knockout mice are characterized by an increased postnatal lethality due to a massive accumulation of autophagosomes in most tissues. Indeed, LAMP2 is required for the fusion of autophagosomes with lysosomes—the final stage of macroautophagy (Chi et al., 2019; Huynh et al., 2007), and LAMP2 was identified as the receptor in the lysosomal membrane for substrate proteins of chaperone-mediated autophagy (Bandyopadhyay et al., 2008). Recently, LAMP2 has also been described to directly bind cholesterol and facilitate its export from lysosomes (Li and Pfeffer, 2016).

In the present study, we investigated the impact of LAMP2 on HSV-1 infection and the AD-like phenotype induced by the virus. To do this, a LAMP2-deficient neuroblastoma cell line was used, in which infection efficiency, Aβ secretion and tau phosphorylation were evaluated. In addition, AD risk of LAMP2 genetic variants was determined in a case-control sample.

2. Materials and methods

2.1. Cell cultures

The murine neuroblastoma N2a cell lines, wild-type (wt) and with a stable knockdown of LAMP2 (LAMP2-), were kindly provided by P. Saftig (Rothaug et al., 2015). N2a cells were cultured in Dulbecco's modified Eagle's medium (DMEM) supplemented with 10% heat-inactivated fetal calf serum, 1 mM sodium pyruvate, 2 mM glutamine and 50 μg/ml gentamycin. To the N2a LAMP2-deficient cells, 400 μg/ml G418 (Invitrogen) was added to the media. All cells were cultured at 37 °C in a 5% CO2 atmosphere.

2.2. Antibodies

Rat anti-mouse LAMP2 was deposited to the Developmental Studies Hybridoma Bank by August, J.T. (DSHB Hybridoma Product ABL-93). Antibodies that recognized viral proteins gC and ICP4 were supplied by Abcam [anti-HSV1 gC Envelope Protein (3G9; ab6509) and anti-HSV 1 ICP4 Immediate Early Protein [10F1]; ab6514). Mouse monoclonal anti-tubulin (clone B-5-1-2; T5168) was obtained from Sigma and phospho-Tau (Thr231) Polyclonal Antibody (44746G) from ThermoFisher Scientific. The secondary antibodies used for immunostaining were horseradish peroxidase-coupled anti-mouse (Vector; PI-2000) and anti-rabbit (Nordic; GAR/IgG (H + L)/PO) antibodies, and donkey anti-Mouse IgG (H + L) antibody coupled to Alexa Fluor 488 (ThermoFisher Scientific; A-21202).

2.3. Infection conditions and plaque assays

The wild-type HSV-1 strain KOS 1.1 was propagated and purified from Vero cells as previously described (Burgos et al., 2002). For the non-synchronized infection at 37 °C, N2a cells seeded in complete DMEM at 70–80% confluency were exposed to HSV-1 at 37 °C for 1 h. For the synchronized infection, cells were incubated at 4 °C for 20 min prior to the incubation with HSV-1 at 4 °C for 1 h. Unbound virus was removed and cells were washed with phosphate-buffered saline (PBS) and then incubated in complete DMEM medium at 37 °C. Mock infections were performed using a virus-free suspension. The multiplicities of infection (moi) used were 0.1, 0.3, 1 or 10 plaque forming units [pfu] per cell. Time and multiplicity of infection are indicated in each experiment.

The infectious titers of purified virus and cell supernatants were determined by plaque assays. Briefly, the titration of serially diluted HSV-1 and cell supernatant samples was performed in Vero cells grown in 24-well plates. Cells were overlain with a mixture of DMEM containing 2% FCS and 0.7% agar. After 48 h the cells were fixed and stained overnight with 1% crystal violet in 5% formaldehyde and the plaques counted.

2.4. Viral DNA quantification

DNA was purified by using the QIAamp® DNA Mini Kit (QIAGEN). The amount of HSV-1 DNA was quantified by real-time quantitative PCR with an ABI Prism 7900HT SD® system (Applied Biosystems) using a custom designed TaqMan probe specific for the US12 viral gene (5′-AGGCGGCCAGAACC-3′). Viral DNA content was then normalized in

terms of mouse genomic DNA, quantified with a predesigned TaqMan probe specific for the *Gapdh* gene (Mm99999915_g1; Applied Biosystems). The quantification data were expressed as viral DNA copy number per ng of genomic DNA.

2.5. Immunofluorescence analysis

Immunofluorescence assays were performed on cells grown on coverslips. Samples were fixed in 4% paraformaldehyde and incubated with the appropriate primary and secondary antibodies. Alexa Fluor 488-coupled antibody was used as a secondary antibody. DAPI (5 mg/ml; Merck) was added 10 min before the end of the procedure to visualize the nuclei. Cells were examined using a Zeiss Axiovert 200 fluorescence microscope. Images were captured by a Spot RT slider digital camera (Diagnostic) using MetaMorphTM imaging software, and processed using Adobe Photoshop package.

2.6. Western blot analysis

To obtain cell lysates, cells were treated with radioimmunoprecipitation assay (RIPA) buffer (10 mM Tris-HCl pH 7.5, 50 mM NaCl, 0.2% sodium deoxycholate, 1% Nonidet P-40%, and 0.1% sodium dodecyl sulfate) containing protease and phosphatase inhibitor cocktails (PhosSTOP, Roche), and incubated for 30 min at 4 °C. Lysates were clarified for centrifugation at 13,000 g for 15 min at 4 °C. Determinations of protein content were performed using the bicinchoninic acid assay (Pierce). Cell lysates were mixed with Laemmli buffer, sonicated, and heated for 5 min at 100 °C. After electrophoretic separation, the gels were blotted onto a nitrocellulose membrane and stained with the appropriate antibodies. A peroxidase-coupled antibody was used as a secondary antibody. Detection by enhanced chemiluminescence was performed using ECL Western blotting detection reagents (Amersham Biosciences) according to the manufacturer's instructions.

2.7. Quantitative RT-PCR

The mRNA transcribed from each gene was quantified by reverse transcription followed by real-time PCR. Briefly, total RNA was isolated with High PureRNA Isolation Kit (Roche) and subjected to reverse transcription using the High Capacity cDNA Archive Kit (Applied Biosystems). Real-time PCR assays for murine *Lamp2* mRNA and for viral ICP0, thymidine kinase (TK) and UL20 mRNAs were designed with the ProbeFinder tool (Roche). cDNAs were amplified by PCR with primers specific to *Lamp2* (forward: 5′-TGCAGAATGGGAGATGAATTT-3'; reverse: 5′-GGCACTATTCCGGTCATCC-3′); ICPO (forward: 5′- AGCGAGTACCCGCCGGCCTG-3'; reverse: 5′- CAGGTCTCGGTCGCAGGGAAAC-3′); TK (forward: 5′- ATACCGACGATCTGCACCT-3'; reverse: 5′-TTATTGCCGTGCGG-3′) and UL20 (forward: 5′- GACGTCCAACAACTCGGTCC-3'; reverse: 5′- GCTCGGCGTTTACGGGA-3′). In the case of murine *Gapdh* gene, RT-PCR was performed using a TaqMan assay (Mm9999995_g1). The data were normalized with respect to the value obtained for the *Gapdh* gene due to its constant expression. Real-time PCR assays were performed in an ABI Prism 7900HT SD system (Applied Biosystems). The quantities of mRNAs were determined using SDS v2.4 software.

2.8. Measurement of secreted Aβ by ELISA

Conditioned media of N2a cells were collected and centrifuged at 1,000 g for 10 min. Viral particles of supernatants were inactivated by ultraviolet irradiation. The media was then assayed for murine Aβ40 and Aβ42 using commercial sandwich enzyme-linked immunosorbent assay (ELISA) kits according to the manufacturer's instructions (WAKO). Aβ amount was quantified measuring the absorbance at 450 nm within 30 min of the completion of the procedure. Values were normalized with the Aβ standard curve and expressed in pM.

2.9. Genetic association study

2.9.1. Study subjects

The study sample included 712 patients with sporadic AD (mean age at onset 72.4 ± 9.0 years; 64.2% women) who met NINCDS/ADRDA criteria for probable AD (McKhann et al., 1984). All AD cases were defined as sporadic because their family history did not mention any first-degree relative with dementia. AD patients were recruited from the Departments of Neurology of the Hospital La Paz (Madrid, Spain), ISCIII Collection (C.0002965) and the Hospital Marqués de Valdecilla (Santander, Spain). Control subjects were 656 unrelated individuals (mean age at examination 76.8 years ± 12.9 years 65% women). These subjects were free of significant illness and had Mini Mental State Examination scores of 27 or more. The controls arose from the same base population as the cases and both groups were of Caucasian origin. All subjects gave their informed consent to be included in the study, which was approved by the Ethics Committees of the participating institutions.

2.9.2. Single nucleotide polymorphism (SNP) selection

TagSNPs were selected to cover 80% of the variability of *LAMP2* gene (ENSEMBL ID ENSG00000005893) in the CEU population (Utah residents with Northern and Western European ancestry) included in the HapMap project. The tagSNPs representative of each haplotype block were chosen based on genotyping probe availability (TaqMan assays from Applied Biosystems), minor allele frequency (MAF>5%), linkage disequilibrium ($r^2 > 0.8$) and, when possible, predicted functional effect. The SNPinfo tool (https://snpinfo.niehs.nih.gov/cgi-bin/snpinfo/snptag.cgi) was used for the selection. For the *LAMP2* gene, an additional SNP in the promoter region (rs42901) was included based on its potential effect on the binding of transcription factors. All selected SNPs are shown in Table 1.

2.9.3. Genotyping

Genotyping was performed with predesigned assays (TaqMan SNPs OpenArrays; Applied Biosystems) according to manufacturer instructions and genotypes were assigned with the TaqMan Genotyper Software (Applied Biosystems).

2.10. Statistical analysis

Graph data are shown as means ± standard error of the mean (SEM).

Table 1
LAMP2 SNPs analysed in the genetic association study.

dbSNP ID[a]	Chr. X position (bp)[b]	Assay ID[c]	Haplotype block[d]	MAF [e]
rs7889047	119576042	C_34815961_10	1	0.37 (*0.40*)
rs42892	119579747	C__2543545_10	2[f]	0.29 (*0.42*)
rs42894	119586729	C__2256955_10	3**	0.21 (*0.15*)
rs2283738	119592386	C_15959427_10	1	0.38 (*0.42*)
rs42901	119605603	C__2543554_10	4	0.30 (*0.15*)

[a] Identification of the SNPs in the dbSNP database.
[b] SNP position in Chromosome X (base pair, bp) in the human genome version hGCR38.p13.
[c] TaqMan genotyping assay code in Applied Biosystems.
[d] Haplotype blocks, defined with a pairwise r^2 cut-off of 0.8 in the CEU population.
[e] Frequency of the minor allele (MAF) in the 1000 Genomes project (human genome version GRCh38.p13). Mean value for the different populations included. In parenthesis, MAF in our study sample.
[f] Partially linked to block 1 and ** to block 4 in Iberian population (r^2 0.63 and r^2 0.56, respectively).

Differences between groups were analysed pairwise using the 2-tailed student t-test. Significance was recorded at $p < 0.05$ (*), $p < 0.01$ (**), and $p < 0.001$ (***). Before analysis, the largest and the smallest variances were tested for homogeneity using the F-test. For the analysis of data expressed as relative values, one sample *t*-test was performed.

Genotype distributions were compared using χ^2 tests and logistic regression models adjusted for age at AD onset, gender and APOE genotype. Interaction between APOE and LAMP2 genotypes were estimated by including an interaction term in the logistic model and by the calculation of the synergy factor as described (Cortina-Borja et al.,

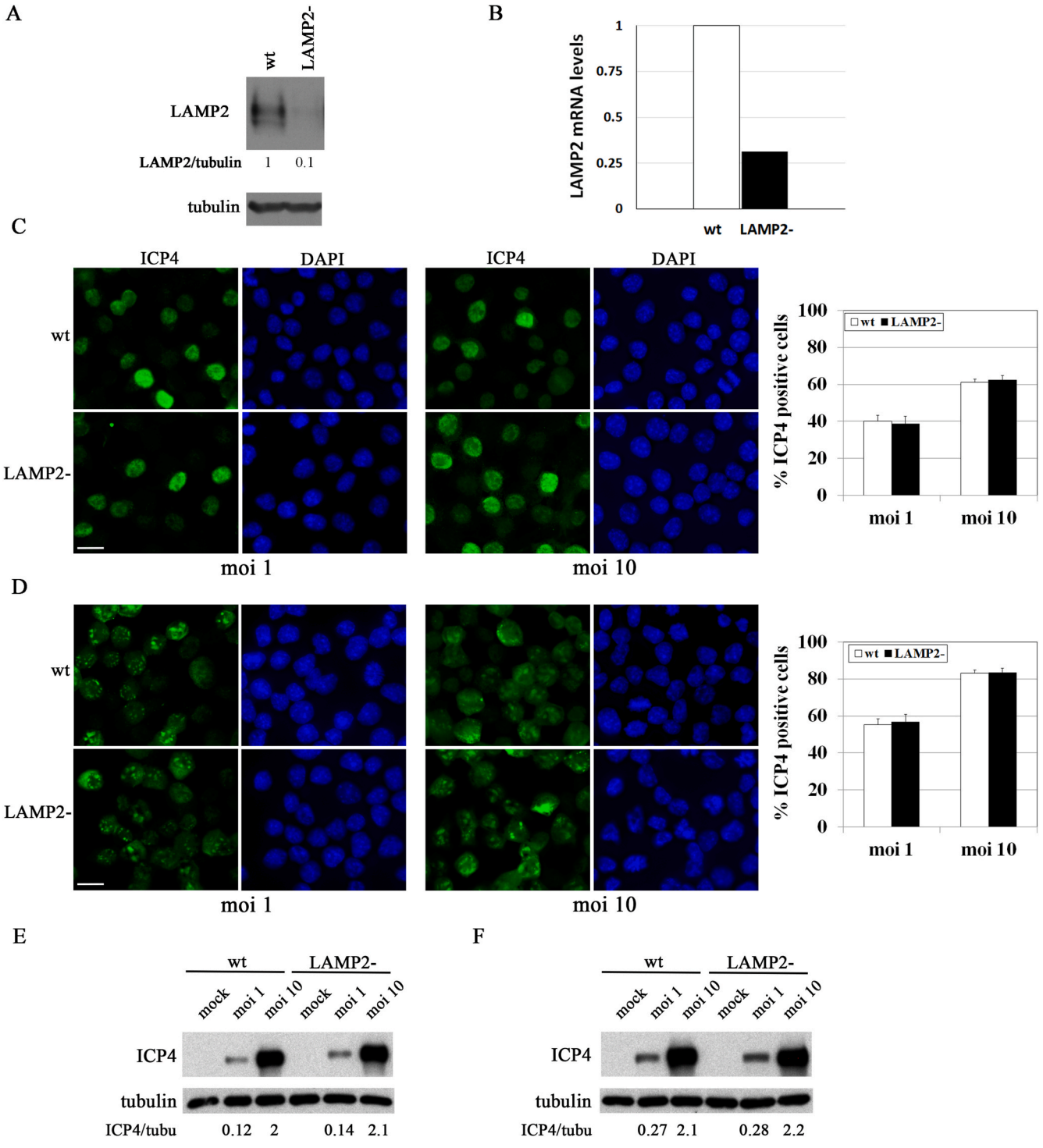

Fig. 1. LAMP2 knockdown does not affect HSV-1 entry. A) Analysis by Western blot of LAMP2 levels in wild-type (wt) and LAMP2-deficient (LAMP2-) N2a cells. The blots shown are representative of three independent experiments. A tubulin blot is provided as a control for equal loading. The ratio of LAMP2 to tubulin with respect to wt cells is shown below the blots. **B)** Quantitative RT-PCR of LAMP2 mRNA levels in wt and LAMP2-deficient N2a cells. Data are expressed as LAMP2 mRNA levels with respect to wt cells. Immunofluorescence analysis of wt and LAMP2-deficient N2a cells infected with HSV-1 at a moi of 1 and 10 pfu/cell for 3 h **(C)** or 5 h **(D)**. The immunoreactivity of ICP4 viral protein is shown. Nuclei are stained with DAPI. Graphs show the percentage of ICP4-positive cells. At least 300 nuclei were counted for each condition. Scale bar: 25 μm. Analysis of ICP4 levels by Western blotting in wt and LAMP2-deficient N2a cells infected with HSV-1 at a moi of 1 and 10 for 3 h **(E)** and 5 h **(F)**. A tubulin blot is provided as a control for equal loading.

2009). Statistical analyses were performed using IBM SPSS Statistics 25 (IBM Corp. IBM SPSS Statistics for Windows. Armonk, NY). Allele and haplotype distributions were examined using Haploview v4.2 software (Barrett et al., 2005) (http://www.broad.mit.edu/mpg/haploview/index.php).

3. Results

3.1. LAMP2 deficiency reduces the efficiency of HSV-1 infection

To evaluate the involvement of LAMP2 in the HSV-1 infection cycle, a murine neuroblastoma N2a cell line with a stable knockdown of LAMP2 was used. First of all, knockdown of LAMP2 was verified by monitoring LAMP2 mRNA and protein levels. Western blot experiments using a specific antibody for the murine LAMP2 protein revealed the decrease (more than 90%) of LAMP2 levels (Fig. 1A). Quantification of LAMP2 mRNA by RT-qPCR confirmed the results obtained by Western blot (Fig. 1B).

The impact of LAMP2 on viral entry was assessed by monitoring the number of HSV-1 infected synchronized cells at early stages of infection by immunofluorescence analysis using a specific antibody for ICP4. ICP4 is coded for by an immediate-early gene, the expression of which begins before HSV-1 DNA replication takes place, and it accumulates in the nucleus of infected cells. Wt and LAMP2-deficient N2a cells were infected at a moi of 1 and 10 for 3 and 5 h. As shown in Fig. 1C and D, the percentage of infected cells was similar in the different infection conditions for both cell lines. These data are consistent with the results obtained in the immunoblotting experiments that showed no changes in total ICP4 levels in wt compared to LAMP2-deficient cells infected with HSV-1 in all conditions tested (Fig. 1E and F). These results indicate that LAMP2 deficiency does not affect viral entry.

Then, we investigated if LAMP2 affected viral stages after HSV-1 entry (e.g. production of late viral proteins, viral DNA replication, viral gene expression or production of infectious particles). To test this hypothesis, the levels of viral glycoprotein C (gC), HSV-1 DNA, viral gene expression of different viral genes and viral titer were monitored at different times and viral doses. When cells were exposed to high viral doses of HSV-1 (moi 1 and 10 for 18 h; similar to an acute infection), an increase of the gC amount in a dose-dependent manner was observed in wt and LAMP2-deficient cells. In addition, LAMP2 deficiency led to lower levels of gC compared to wt cells, only when cells were infected at the lower dose (moi 1) (Fig. 2A). When gC levels were assessed in cells infected at low viral doses for longer (moi 0.1 or 0.3 for 24 or 42 h; a situation more like that of natural HSV-1 infection), the alteration of gC levels was greater than in the previous conditions, and a significant decrease in gC levels was recorded in LAMP2-deficient cells in all conditions tested (Fig. 2B and C). gC is a γ2 "true late'' gene which expression strictly depends on viral DNA synthesis. The decrease in gC levels in LAMP2-deficient cells could therefore indicate altered viral replication and motivated us to further analyse viral DNA levels and the production of infectious particles. The quantification of viral DNA revealed that LAMP2-deficient cells contained less viral DNA in all conditions tested (Fig. 3A). Interestingly, gC and viral DNA amount was specially reduced at 24 and 42 h of infection, times at which at least one replication cycle has been completed. Then, the role of LAMP2 in the expression of viral genes was evaluated by measuring the levels of mRNA of ICP0 (immediate early gene), thymidine kinase (TK; early gene) and UL20 (late gene) at 24 and 42 h postinfection (Fig. 3B and C). A marked decrease of the expression of all viral genes was recorded in LAMP2-deficient cells. Finally, the effect of LAMP2 on the production of infectious particles was examined by plaque assays. A reduction in the extracellular viral titers was also observed in LAMP2-deficient cells (Fig. 3D).

Taken together, these results indicate that low levels of LAMP2 reduces the efficiency of HSV-1 infection and suggest an effect of this protein in a late stage of the viral cycle.

3.2. LAMP2 deficiency attenuates the neurodegeneration markers induced by HSV-1

With the aim of assessing the impact of LAMP2 on the neurodegeneration markers induced by HSV-1, the levels of phosphorylated tau and amyloid-β peptide (Aβ) were monitored in wt and LAMP2-deficient N2a cells.

First, tau phosphorylation in the epitope thr231, which is known to be phosphorylated in AD brains and in HSV-infected cells (Kristen et al.,

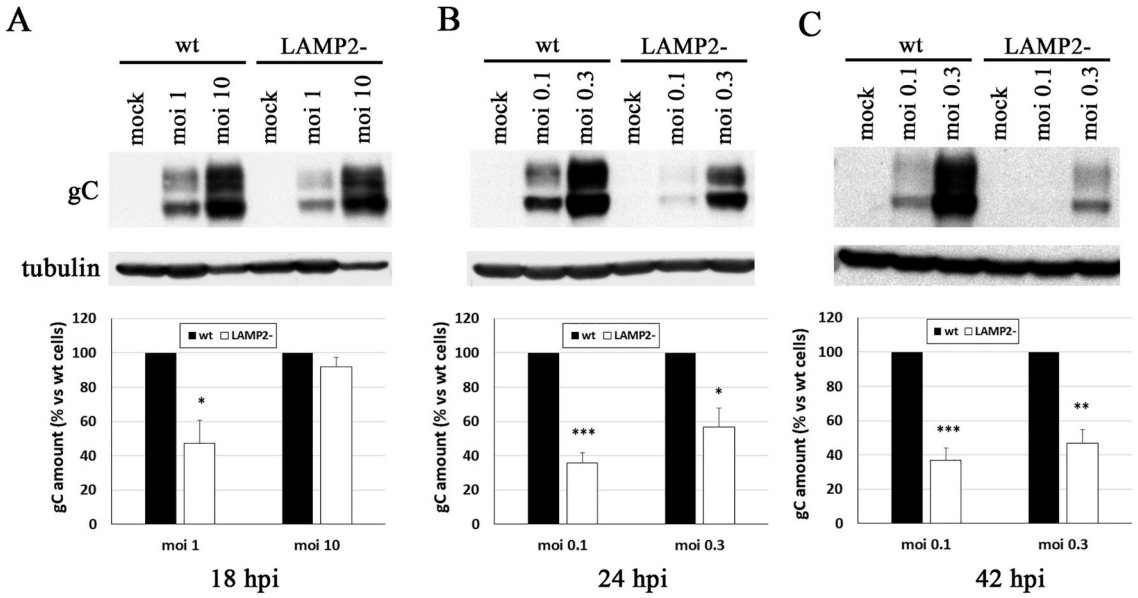

Fig. 2. LAMP2 knockdown reduces the amount of viral glycoprotein C at different infection conditions. Levels of viral glycoprotein C (gC) were monitored at different times of infection and viral doses by Western blot analysis in wt and LAMP2-deficient N2a cells infected with HSV-1. A tubulin blot is provided as a control for equal loading. **A)** N2a cells were infected with HSV-1 at a moi of 1 and 10 pfu/cell for 18 h (hpi, hours post-infection). N2a cells were also infected at lower viral doses (moi 0.1 and moi 0.3 pfu/cell) for 24 hpi **(B)** and 42 hpi **(C)**. In all graphs, data represent the mean ± SEM of at least three experiments and are expressed as a percentage with respect to wt N2a cells (one sample *t*-test; *p < 0.05; **p < 0.01; ***p < 0.001).

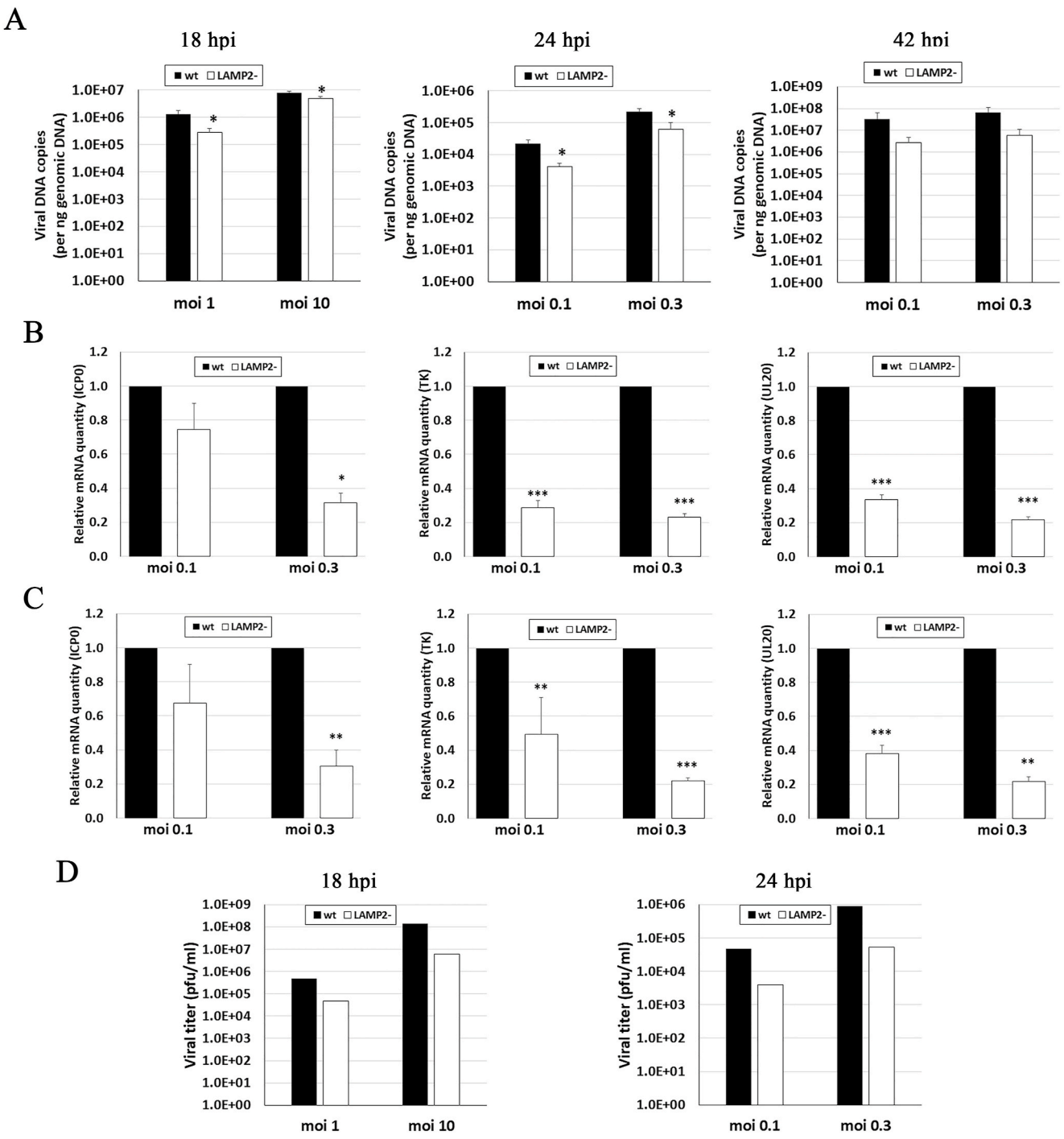

Fig. 3. LAMP2 knockdown led to the decrease of viral DNA levels, viral gene expression and infectious particle production. A) Wt and LAMP2-deficient N2a cells were infected with different viral doses and the amount of viral DNA was analysed by quantitative PCR at different times post-infection (18, 24 and 42 hpi). The data represent the mean ± SEM of at least five experiments performed in triplicate (Student *t*-test; *$p < 0.05$). Wt and LAMP2-deficient N2a cells were exposed to HSV-1 at a moi of 0.1 and 0.3 pfu/cell for 24 h **(B)** or 42 h **(C)** and mRNA levels of ICP0, thymidine kinase (TK) and UL20 viral genes were determined by quantitative RT-PCR, and normalized by the levels of *Gapdh* mRNA. The data represent the mean ± SEM of two experiments performed in triplicate and are expressed as the relative value respect to wt cells (one sample *t*-test; *$p < 0.05$; **$p < 0.01$; ***$p < 0.001$). **D)** Extracellular viral titers were measured in wt and LAMP2-deficient N2a cells infected with HSV-1 at a moi of 1 and 10 pfu/cell for 18 h, or at a moi of 0.1 and 0.3 for 24 h. A representative experiment is shown.

2015), was evaluated. We found an increase of tau phosphorylation in infected N2a cells, which is much higher in wt than in LAMP2-deficient cells (Fig. 4A). The effect of LAMP2 deficiency on tau phosphorylation was also studied. No effect was seen in non-infected cells. In contrast, a significant reduction of the levels of phosphorylated tau was found in LAMP2-deficient cells exposed to HSV-1 (Fig. 4B), suggesting that LAMP2 deficiency partially blocks the effect provoked by the virus.

Our group previously reported that HSV-1 caused the accumulation of intracellular Aβ in human neuronal cells, and this process was partly mediated by a decreased efficiency of the secretion of this peptide (Santana et al., 2012b). Therefore, the levels of secreted Aβ40 and Aβ42 were measured by ELISA. As expected, HSV-1 caused a marked reduction in both Aβ species in N2a cells (Fig. 5A). When the effect of LAMP2 was analysed, an increase of the levels of secreted Aβ was recorded in

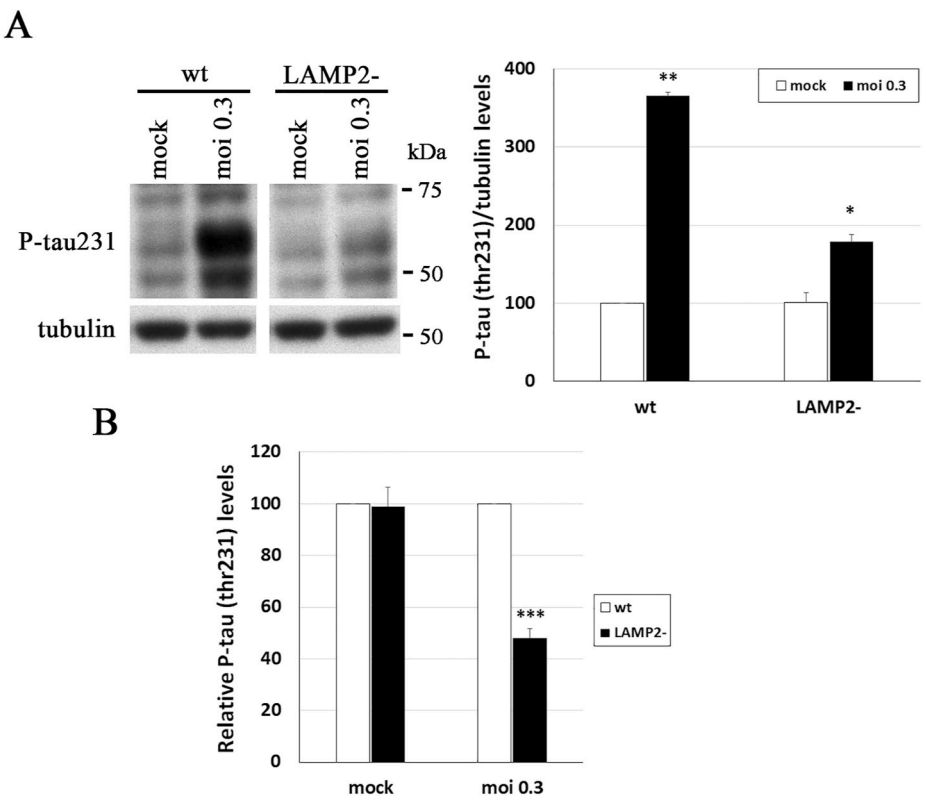

Fig. 4. LAMP2 knockdown reduces phosphorylated tau levels in HSV-1-infected cells. Wt and LAMP2-deficient N2a cells were infected with HSV-1 at a moi of 0.3 pfu/cell for 42 h. **A)** HSV-1 induces an increase of phosphorylated tau levels. Tau phosphorylation was evaluated by Western blot analysis using an antibody specific for the epitope thr231 (P-tau231). A tubulin blot is provided as a control for equal loading. Graph data represent the mean ± SEM of four independent experiments and are expressed as a percentage with respect to non-infected (mock) wt cells (one sample *t*-test; *p < 0.05; **p < 0.01). **B)** LAMP2 deficiency reduces tau phosphorylation in HSV-1-infected cells. Graph data represent the mean ± SEM of four independent experiments and are expressed as a percentage with respect to wt cells (one sample *t*-test; ***p < 0.001).

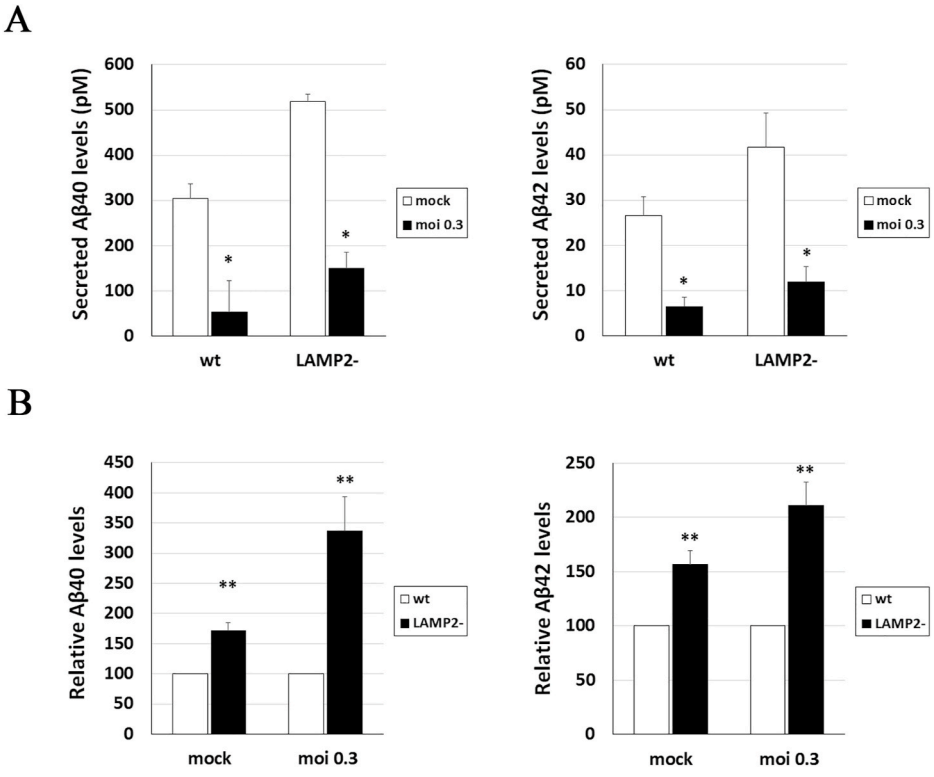

Fig. 5. LAMP2 attenuates the inhibition of Aβ secretion induced by HSV-1. Wt and LAMP2-deficient N2a cells were infected with HSV-1 at a moi of 0.3 pfu/cell for 42 h and conditioned media were used to determine the levels of extracellular Aβ40 and Aβ42 peptides by ELISA assays. **A)** HSV-1 inhibits Aβ secretion. Graph data are expressed in pM and represent the mean ± SEM of seven independent experiments (student t-test; *p < 0.05). **B)** LAMP2 deficiency increases Aβ secretion. Graph data represent the mean ± SEM of seven independent experiments and are expressed as a percentage with respect to wt cells (one sample *t*-test; **p < 0.01).

LAMP2-deficient cells (Fig. 5B). Importantly, this augment was higher in cells exposed to HSV-1 pointing to an effect more pronounced of LAMP2 in infected cells.

Taken these findings together, LAMP2 deficiency partially reverts the increase of phosphorylated tau and inhibition of Aβ secretion observed in infected cells, suggesting a functional role of LAMP2 in the appearance of the AD-like phenotype induced by HSV-1.

3.3. Genetic association of LAMP2 gene with AD

We next tested if the involvement of LAMP2 in the neurodegeneration observed in the infection cell models could be validated in AD patients. To this aim, SNPs in *LAMP2* gene were selected, and their association with sporadic AD investigated in the case/control sample described in Methods. First, the tagSNPs originally chosen from the HapMap CEU population as described in Methods were restudied in the Iberian population included in the 1000 Genomes project located in the ENSEMBL server (human genome version GRCh38.p13) (http://www.ensembl.org/Homo_sapiens/Info/Index?db=core). We found no major differences in the haplotype architecture between the Iberian and CEU populations indicating that the selected tagSNPs were actually valid for our study sample. However, some exceptions were found, like stronger linkage disequilibrium between the LAMP2 SNPs rs7889047 and rs42892 in the Iberian (pairwise r^2 0.62) compared to the CEU population (r^2 0.35), illustrating the genetic architecture background variation among populations. The APOE genotype of these subjects had been previously analysed (Recuero et al., 2009; Rodriguez-Rodriguez et al., 2010). The study of the individual genotypes was performed in the whole sample and in the sample stratified by gender, since *LAMP2* is a gene located in the X chromosome. As shown in Table 2, the analysis revealed a significant association of the SNPs of haplotype block 1 (rs7889047 and rs2283738) in males, and of the SNP rs42898 in females. After adjusting for age at onset and APOE genotype in logistic regression models, the association of rs2283738 with AD in males remained significant ($p = 0.005$).

We next looked for possible interactions of the LAMP2 SNPs with APOE-*ε4* genotype by including interaction terms in the logistic regression models and by sample stratification followed by the calculation of synergy factor as described (Cortina-Borja et al., 2009). No significant associations or interactions were found in women. By contrast, in men there was a trend for a stronger association in those carrying the APOE4 allele for all the LAMP2 SNPs (Table 3). This difference was significant for the SNPs rs7889047: odds ratio 1.37 in APOE4 non carriers and 4.40 in the carriers; Cochran & Mantel-Haenszel test of conditional independence $p < 0.05$; synergy factor 3.22 (95% CI 1.05–9.95; p 0.04) and for rs2283738: odds ratio 1.41 and 6.02 respectively; Cochran & Mantel-Haenszel $p < 0.05$; synergy factor 4.27 (95% CI 1.42–12.83; p 0.01). The interaction term between rs2283738 and APOE genotype included in the logistic regression contributed significantly to the model ($p = 0.005$).

4. Discussion

Our group has been engaged during several years in developing a neuronal cell model of HSV-1 infection with the aim of studying the implication of this virus in AD. We have reported HSV-1 to modify tau phosphorylation (Alvarez et al., 2012), APP proteolytic processing (Santana et al., 2012b), and autophagy (Santana et al., 2012a), all of which have been associated with the pathogenesis of AD. Lysosomal pathway has been tightly linked with AD over the last decades (Whyte et al., 2017). In line with this, gene differential expression analysis of our cell model of infection revealed that the main process altered was the lysosomal system, and the gene encoding for the lysosomal membrane protein LAMP2 was, among potential mediators of the lysosomal dysfunction induced by the infection, the most highly upregulated one. Further functional studies revealed that HSV-1 infection increased lysosomal load, reduced the activity of lysosomal hydrolases and altered endocytosis pathway (Kristen et al., 2018). These findings led us to focus on LAMP2 as the strongest candidate to be involved in the AD-like phenotype induced by the virus.

The role of LAMP2 during HSV-1 infection has remained unexplored. In order to investigate whether LAMP2 is involved in the HSV-1 viral cycle, a murine neuroblastoma N2a cell line with a stable knockdown of LAMP2 was used, and the different stages involved in the infection

Table 2
Genotype distributions in the case/control sample stratified by gender.

SNP ID			Genotype[a]			p (χ^b)[b]
rs7889047			A A	A G	G G	
Total	Control	533	253 (0.47)	118 (0.22)	162 (0.30)	
	AD	554	293 (0.53)	120 (0.23)	141 (0.22)	
Male	Control	168	90 (0.54)		78 (0.46)	0.012
	AD	202	134 (0.66)		68 (0.34)	
Female	Control	365	163 (0.45)	118 (0.32)	84 (0.23)	
	AD	352	159 (0.45)	120 (0.34)	73 (0.21)	
rs42892			**C C**	**C T**	**T T**	
Total	Control	516	161 (0.31)	99 (0.19)	256 (0.50)	
	AD	504	161 (0.32)	106 (0.21)	237 (0.47)	
Male	Control	175	64 (0.37)		111 (0.63)	
	AD	184	83 (0.45)		101 (0.55)	
Female	Control	341	97 (0.28)	99 (0.29)	145 (0.43)	
	AD	320	78 (0.24)	106 (0.33)	136 (0.43)	
rs42894			**A A**	**A T**	**T T**	
Total	Control	574	451 (0.79)	77 (0.13)	46 (0.08)	
	AD	622	455 (0.73)	116 (0.19)	51 (0.08)	
Male	Control	180	158 (0.88)		22 (0.12)	
	AD	216	181 (0.84)		35 (0.16)	
Female	Control	394	293 (0.74)	77 (0.20)	24 (0.06)	0.007
	AD	406	274 (0.66)	116 (0.29)	16 (0.04)	
rs2283738			**A A**	**A G**	**G G**	
Total	Control	602	166 (0.28)	180 (0.30)	256 (0.43)	
	AD	613	147 (0.24)	168 (0.27)	298 (0.49)	
Male	Control	195	89 (0.46)		106 (0.54)	**0.008**[c]
	AD	221	73 (0.33)		148 (0.67)	
Female	Control	407	77 (0.19)	180 (0.44)	150 (0.37)	
	AD	392	74 (0.19)	168 (0.43)	150 (0.38)	
rs42901			**A A**	**A T**	**T T**	
Total	Control	571	45 (0.08)	79 (0.14)	447 (0.78)	
	AD	596	55 (0.09)	102 (0.17)	439 (0.74)	
Male	Control	189	26 (0.14)		163 (0.86)	
	AD	209	38 (0.18)		171 (0.82)	
Female	Control	382	19 (0.05)	79 (0.21)	284 (0.74)	
	AD	387	17 (0.04)	102 (0.26)	268 (0.70)	
APOE4 alleles			**0**	**1**	**2**	
Total	Control	656	543 (0.83)	113 (0.17)	0	**5.4E-42**[c]
	AD	721	341 (0.47)	371 (0.52)	9 (0.01)	
Male	Control	220	187 (0.85)	33 (0.15)	0	**1.3E-19**[c]
	AD	258	113 (0.44)	140 (0.54)	5 (0.02)	

(*continued on next page*)

Table 2 (*continued*)

SNP ID			Genotype[a]			p (χ^{b})[b]
rs7889047			A A	A G	G G	
Female	Control	436	356 (0.82)	80 (0.18)	0	**1.9E-23**[c]
	AD	463	228 (0.49)	231 (0.50)	4 (0.01)	

[a] The number of individuals with the frequency in parenthesis is shown.
[b] p value for the 2-sided Pearson χ^{b} test.
[c] Association remaining significant in the logistic regression analyses.

process were evaluated. LAMP2 has been recently reported to act as a receptor for Tripanosoma cruzi cell invasion (Rodrigues et al., 2019). Thus, as a first characterization step, the impact of LAMP2 deficiency on HSV-1 entry was analysed. No effects were observed on viral entry in LAMP2-knockdown cells. However, all the events that require DNA synthesis were impaired, such as expression of true late γ2 proteins, viral DNA replication itself, or infectious viral particle production, suggesting that the role of LAMP2 may be related to DNA replication. In addition, the inhibition of the formation of new infectious particles in LAMP2-deficient cells was much stronger than the inhibition of viral DNA replication, suggesting that an additional defect in a late stage of infection might occur (e.g. maturation of viral particle). In this respect, HSV proteins involved in virus assembly and envelopment, including HSV-1 glycoprotein B and HSV-2 UL56, have been found to colocalize with CD63, another lysosomal membrane protein (Temme et al., 2010; Ushijima et al., 2009). These findings indicate that LAMP2 knockdown severely affects the HSV-1 viral cycle and, therefore, could impact on the neurodegeneration markers induced by the virus.

The neurodegenerative effects of HSV-1 infection in human neuronal cells are well known by our group (Alvarez et al., 2012; Santana et al., 2012a, 2012b). To determine if these effects can be reproduced in murine N2a cells and evaluate if a differential response in LAMP2-deficient cells takes place, we started analysing the levels of secreted Aβ and phosphorylated tau in these cell models. HSV-1 infection provoked increased levels of phosphorylated tau, inhibition of Aβ secretion and accumulation of intracellular Aβ and the autophagic marker LC3-II (unpublished results). Thus, N2a cells fully recapitulate the pathological markers found in HSV-1 infected human neuronal cells, and are appropriate to assess the role of LAMP2 in the HSV-1-induced neurodegeneration.

In this work, LAMP2 deficiency impaired HSV-1 infection, particularly in chronic infection conditions—low viral dose and longer time, a situation more like that of natural HSV-1 infection. The fact that LAMP2 deficiency causes a lower production of infectious particles indicates that, if LAMP2 is implicated in HSV-1-mediated neurodegeneration, changes might be observed at later time points when a full replication cycle has been completed. Indeed, our data indicated that LAMP2 deficiency significantly attenuates the neurodegenerative effects—increase of phosphorylated tau and inhibition of Aβ secretion—induced by HSV-1 in chronic conditions. The question arises as to whether the attenuation of neurodegeneration events provoked by LAMP2 deficiency is merely due to the inhibition of infection observed in LAMP2-deficient cells. However, several findings points out an active role of LAMP2 in infected cells: i) LAMP2 knockdown also significantly increases Aβ secretion in non-infected cells, indicating an effect of LAMP2 independently of HSV-1 infection; ii) our group has previously reported that the intracellular accumulation of Aβ and the inhibition of its secretion in human neuronal cells is not affected by the inhibition of viral replication (Santana et al., 2012b), and iii) we found that oxidative stress is able to increase the neurodegeneration markers induced by the virus although it impairs HSV-1 infection (Santana et al., 2013).

LAMP2 has been functionally involved in the export of cholesterol out of late endosomes and lysosomes (Li and Pfeffer, 2016; Schneede et al., 2011) and in the fusion of autophagosomes with lysosomes—the final stage of autophagy—(Huynh et al., 2007). Both processes are essential for lysosome function and have been reported to be deeply altered in numerous neurodegenerative diseases, including AD (Djelti et al., 2015; Van Acker et al., 2019), and are also impaired by HSV-1 infection (Hsu et al., 1995; O'Connell and Liang, 2016). In addition, alterations of cholesterol homeostasis and autophagic process have been reported to induce the accumulation of hyperphosphorylated tau and intracellular Aβ (Barbero-Camps et al., 2018; Reddy and Oliver, 2019; van der Kant et al., 2019). Finally, LAMP2 loss-of-function mutations cause Danon disease, a X-linked disorder characterized by hypertrophic cardiomyopathy, myopathy and intellectual disabilities in which there is an accumulation of immature autophagic vesicles and prominent storage of lysosomal cholesterol (Endo et al., 2015). Taken these findings together, LAMP2 deficiency could cause cholesterol and/or lysosomal alterations which in turn could have consequences on phosphorylated tau and Aβ levels in HSV-1-infected cells. Further investigations are needed to better understand the basic mechanisms involved in these alterations.

Particularly interesting is that LAMP2 has been described to interact with several viral proteins—neuroaminidase from influenza A (Ju et al., 2015), tat (trans-activator of transcription) protein from HIV (Fields et al., 2015), and MuV-F protein from Mumps virus (Ueo et al., 2020)—causing impairment of lysosomal activity. In this context, alterations of lysosomal cholesterol homeostasis and/or autophagosome maturation and lysosomal proteolysis mediated by modification of LAMP2 function by HSV-1 proteins could be involved in the AD-like phenotype induced

Table 3
AD risk associated with LAMP2 SNPs in the sample stratified by gender and APOE genotype. Odds ratios (OR) for the association of Alzheimer's disease with the indicated allele or haplotype in different sample strata defined by gender and APOE genotypes. †The number of individuals (cases/controls) in each stratum is shown. ‡The p-value for the X^2 test is shown in parenthesis. *ns*, non-significant. The study was performed with Haploview 4.2. software.

dbSNP ID	Risk allele	Odds ratio (*p-value*)					
		Women			Men		
		All (407/390) †	APOE4 -(334/73)	APOE4+ (199/191)	All (208/185)	APOE4 -(89/161)	APOE4+ (117/30)
rs7889047	**A**	1.08 (*ns*)‡	1.03 (*ns*)	1.02 (*ns*)	**1.77 (*0.008*)**	1.37 (*ns*)	**4.40 (*0.002*)**
rs42892	C	0.91 (*ns*)	0.80 (*ns*)	0.81 (*ns*)	1.52 (*ns*)	1.09 (*ns*)	**5.78 (*0.003*)**
rs42894	T	1.16 (*ns*)	1.42 (*0.03*)	1.07 (*ns*)	1.34 (*ns*)	1.16 (*ns*)	2.20 (*ns*)
rs2283738	**G**	1.02 (*ns*)	1.10 (*ns*)	1.43 (*ns*)	**1.97 (*0.001*)**	1.41 (*ns*)	**6.02 (7.8E-5)**
rs42901	A	1.10 (*ns*)	1.41 (*0.04*)	1.38 (*ns*)	1.43 (*ns*)	1.55 (*ns*)	3.99 (*ns*)
Block 1	Haplotype						
rs7889047- rs2283738	**AG**	1.11 (ns)	1.13 (ns)	0.77 (ns)	**3.43 (0.002)**	1.98 (ns)	**20.4 (5.0E-4)**
	GA	Ref	Ref	Ref	Ref	Ref	Ref
	GG	0.75 (ns)	0.64 (ns)	2.94 (ns)	2.40 (ns)	1.31 (ns)	21.9 (ns)
	AA	0.93 (ns)	0.67 (ns)	0.82 (ns)	1.10 (ns)	1.21 (ns)	0.95 (ns)

In sum, this study shows that LAMP2 genetic variants—especially in haplotype block 1—are associated with AD in males, with increased risk for APOE-*ε4* carriers, suggesting that LAMP2, most probably integrated into "epistatic mechanisms", is a genetic risk factor for AD.

by HSV-1. To our knowledge, no interactions between herpesvirus proteins and LAMP2 have been reported. The fact that LAMP2 deficiency causes a less effective infection and attenuates the neurodegeneration markers induced by the virus, however, might suggest otherwise. To test this, we have initiated a study of mass spectrometry-based proteomics to analyse the viral interactome of LAMP2. Preliminary results revealed the detection of specific proteins putatively interacting with LAMP2 in infected cells (unpublished results). Thus, identifying the interactome of LAMP2 during HSV-1 infection could offer clues about the role of LAMP2 in the viral cycle and in the appearance of the AD-like phenotype induced by the virus.

LAMP1 and LAMP2 exhibit considerable sequence homology and have high structural similarity (Eskelinen et al., 2003). Consistent with the notion that LAMP1 and LAMP2 may have redundant function, deletion of both genes cause embryonic lethality whereas mice deficient in either LAMP1 or LAMP2 are viable and fertile (Eskelinen, 2006). Further, it has been reported that fibroblasts lacking either LAMP1 or LAMP2 are able to engulf and eliminate *Neisseria gonorrhoeae*. However, LAMP1/LAMP2 double deficient fibroblasts showed arrested maturation of phagosomes containing bacteria and consequently failed to kill the engulfed pathogen (Binker et al., 2007). If LAMP2 was functionally involved in the AD-like phenotype induced by HSV-1, the attenuation of neurodegeneration markers observed in LAMP2 knockdown cells would be consistent with the upregulation of LAMP2 provoked by the infection (Kristen et al., 2018). Moreover, it is tempting to speculate that this attenuation of the AD-like phenotype may be due to the fact that LAMP1 is able to partially compensate the loss of LAMP2. Experiments in LAMP1/LAMP2 double deficient cells would be valuable to confirm this hypothesis.

So far, the results obtained in this work are drawn from in vitro experiments with cell models of infection mimicking sporadic AD. An important question is whether LAMP2 is involved in AD. Genetic association studies of case/control samples were used to validate some in vitro results with actual data from AD patients and revealed the implication of LAMP2 in AD confirming the outcome of our cell model experiments. Our results showed significant association for LAMP2 with males, with increased risk for APOE-ε4 carriers. To increase the statistical power of the sample, the study of the candidate SNPs will be extended to an additional sample of 10,000 cases/controls, available through our association to Dementia Genetics Spanish Consortium (DEGESCO) (Moreno-Grau et al., 2019).

Recurrent evidence on gender differences in the prevalence and clinical expression of AD has been reported (Genin et al., 2011; Lin et al., 2015). In addition, HSV-1 also seems to affect more severely to females (Itzhaki, 2014; Klein, 2012). Interestingly, *LAMP2* gene is coded in the X chromosome. In this context, our findings point to a potential molecular mechanism involved in the consistently reported gender difference on genetic susceptibility to AD. It is tempting to speculate that the higher AD risk in men observed in our population, could be attributed, at least partially, to the fact that males are hemizygous for LAMP2. In this sense, the role of autophagy in some paradigmatic human diseases, including neurodegenerative diseases, has been reported to be gender-dependent (Lista et al., 2011). Further, neurons from males exposed to nutrient starvation more readily undergo autophagy and die, whereas neurons from females mobilize fatty acids, accumulate triglycerides, form lipid droplets and survive longer, suggesting that autophagic response could be gender and tissue specific (Du et al., 2009). LAMP2 could be involved in these gender specific defects since this protein plays an important role in the autophagic process. Although more data are needed to confirm our current genetic association results, the study of the molecular basis of gender differences in AD prevalence and clinical expression is undoubtedly of great interest.

5. Conclusions

In summary, we have analysed the role of LAMP2 in the efficiency of HSV-1 infection and in the appearance of the neurodegeneration markers induced by the virus. Our data showed that LAMP2 knockdown significantly reduces HSV-1 infection and partially attenuates the neurodegeneration events induced by the virus, reducing the phosphorylation of tau and increasing Aβ secretion. In addition, *LAMP2* gene is associated with a higher risk for AD in APOE-*ε4* carrier males. Taking these results into account, LAMP2 could constitute a viral target and the modification of LAMP2 function by the infection may mediate the AD-like phenotype induced by HSV-1.

CRediT authorship contribution statement

Henrike Kristen: Conceptualization, Investigation. **Isabel Sastre:** Methodology, Investigation. **Sara Aljama:** Visualization, Investigation. **Maria Fuentes:** Visualization, Investigation. **Maria Recuero:** Investigation. **Ana Frank-García:** Supervision, Resources. **Angel Martin:** Resources. **Pascual Sanchez-Juan:** Supervision, Resources. **Carmen Lage:** Resources. **Maria J. Bullido:** Formal analysis, Writing – original draft. **Jesus Aldudo:** Visualization, Writing – review & editing.

Declaration of competing interest

The authors declare that they have no known competing financial interests or personal relationships that could have appeared to influence the work reported in this paper.

Acknowledgements

This work was supported by the Spanish *Ministerio de Ciencia e Innovación* (SAF 2017-85747-R); and the Ramon Areces Foundation. The funding sources had no role in study design, collection, analysis and interpretation of data, in writing of the report or the decision to submit for publication. Henrike Kristen is recipient of a UAM-CSIC International Excellence Campus research contract. Institutional grants from the *Fundación Ramón Areces* and *Banco de Santander* to the *CBMSO* are also acknowledged.

References

Abrahamson, E.E., et al., 2020. Modeling Abeta42 accumulation in response to herpes simplex virus 1 infection: 2D or 3D? J. Virol. Dec 2:JVI.02219-20 https://doi.org/10.1128/JVI.02219-20.

Alvarez, G., et al., 2012. Herpes simplex virus type 1 induces nuclear accumulation of hyperphosphorylated tau in neuronal cells. J. Neurosci. Res. 90, 1020–1029. https://doi.org/10.1002/jnr.23003.

Ashraf, G.M., et al., 2019. The possibility of an infectious etiology of alzheimer disease. Mol. Neurobiol. 56, 4479–4491. https://doi.org/10.1007/s12035-018-1388-y.

Bandyopadhyay, U., et al., 2008. The chaperone-mediated autophagy receptor organizes in dynamic protein complexes at the lysosomal membrane. Mol. Cell Biol. 28, 5747–5763. https://doi.org/10.1128/MCB.02070-07.

Barbero-Camps, E., et al., 2018. Cholesterol impairs autophagy-mediated clearance of amyloid beta while promoting its secretion. Autophagy 14, 1129–1154. https://doi.org/10.1080/15548627.2018.1438807.

Barrett, J.C., et al., 2005. Haploview: analysis and visualization of LD and haplotype maps. Bioinformatics 21, 263–265. https://doi.org/10.1093/bioinformatics/bth457.

Binker, M.G., et al., 2007. Arrested maturation of Neisseria-containing phagosomes in the absence of the lysosome-associated membrane proteins, LAMP-1 and LAMP-2. Cell Microbiol. 9, 2153–2166. https://doi.org/10.1111/j.1462-5822.2007.00946.x.

Burgos, J.S., et al., 2002. Involvement of apolipoprotein E in the hematogenous route of herpes simplex virus type 1 to the central nervous system. J. Virol. 76, 12394–12398. https://doi.org/10.1128/jvi.76.23.12394-12398.2002.

Cairns, D.M., et al., 2020. A 3D human brain-like tissue model of herpes-induced Alzheimer's disease. Sci Adv 6, eaay8828. https://doi.org/10.1126/sciadv.aay8828.

Cenini, G., et al., 2020. Dissecting Alzheimer's disease pathogenesis in human 2D and 3D models. Mol. Cell. Neurosci. 110, 103568. https://doi.org/10.1016/j.mcn.2020.103568.

Cortina-Borja, M., et al., 2009. The synergy factor: a statistic to measure interactions in complex diseases. BMC Res. Notes 2, 105. https://doi.org/10.1186/1756-0500-2-105.

Chi, C., et al., 2019. LAMP-2B regulates human cardiomyocyte function by mediating autophagosome-lysosome fusion. Proc. Natl. Acad. Sci. U. S. A. 116, 556–565. https://doi.org/10.1073/pnas.1808618116.

D'Aiuto, L., et al., 2019. Modeling herpes simplex virus 1 infections in human central nervous system neuronal cells using two- and three-dimensional cultures derived

from induced pluripotent stem cells. J. Virol. 93 https://doi.org/10.1128/JVI.00111-19.
Djelti, F., et al., 2015. CYP46A1 inhibition, brain cholesterol accumulation and neurodegeneration pave the way for Alzheimer's disease. Brain 138, 2383–2398. https://doi.org/10.1093/brain/awv166.
Du, L., et al., 2009. Starving neurons show sex difference in autophagy. J. Biol. Chem. 284, 2383–2396. https://doi.org/10.1074/jbc.M804396200.
Eimer, W.A., et al., 2018. Alzheimer's disease-associated beta-amyloid is rapidly seeded by herpesviridae to protect against brain infection. Neuron 99, 56–63. https://doi.org/10.1016/j.neuron.2018.06.030 e3.
Endo, Y., et al., 2015. Danon disease: a phenotypic expression of LAMP-2 deficiency. Acta Neuropathol. 129, 391–398. https://doi.org/10.1007/s00401-015-1385-4.
Eskelinen, E.L., 2006. Roles of LAMP-1 and LAMP-2 in lysosome biogenesis and autophagy. Mol. Aspect. Med. 27, 495–502. https://doi.org/10.1016/j.mam.2006.08.005.
Eskelinen, E.L., et al., 2003. At the acidic edge: emerging functions for lysosomal membrane proteins. Trends Cell Biol. 13, 137–145. https://doi.org/10.1016/s0962-8924(03)00005-9.
Fields, J., et al., 2015. HIV-1 Tat alters neuronal autophagy by modulating autophagosome fusion to the lysosome: implications for HIV-associated neurocognitive disorders. J. Neurosci. 35, 1921–1938. https://doi.org/10.1523/JNEUROSCI.3207-14.2015.
Genin, E., et al., 2011. APOE and Alzheimer disease: a major gene with semi-dominant inheritance. Mol. Psychiatr. 16, 903–907. https://doi.org/10.1038/mp.2011.52.
Hsu, H.Y., et al., 1995. Altered cholesterol trafficking in herpesvirus-infected arterial cells. Evidence for viral protein kinase-mediated cholesterol accumulation. J. Biol. Chem. 270, 19630–19637. https://doi.org/10.1074/jbc.270.33.19630.
Huynh, K.K., et al., 2007. LAMP proteins are required for fusion of lysosomes with phagosomes. EMBO J. 26, 313–324. https://doi.org/10.1038/sj.emboj.7601511.
Itzhaki, R.F., 2014. Herpes simplex virus type 1 and Alzheimer's disease: increasing evidence for a major role of the virus. Front. Aging Neurosci. 6, 202. https://doi.org/10.3389/fnagi.2014.00202.
Itzhaki, R.F., et al., 1997. Herpes simplex virus type 1 in brain and risk of Alzheimer's disease. Lancet 349, 241–244. https://doi.org/10.1016/S0140-6736(96)10149-5.
Ju, X., et al., 2015. Neuraminidase of influenza A virus binds lysosome-associated membrane proteins directly and induces lysosome rupture. J. Virol. 89, 10347–10358. https://doi.org/10.1128/JVI.01411-15.
Klein, S.L., 2012. Sex influences immune responses to viruses, and efficacy of prophylaxis and treatments for viral diseases. Bioessays 34, 1050–1059. https://doi.org/10.1002/bies.201200099.
Kristen, H., et al., 2015. Herpes simplex virus type 2 infection induces AD-like neurodegeneration markers in human neuroblastoma cells. Neurobiol. Aging 36, 2737–2747. https://doi.org/10.1016/j.neurobiolaging.2015.06.014.
Kristen, H., et al., 2018. The lysosome system is severely impaired in a cellular model of neurodegeneration induced by HSV-1 and oxidative stress. Neurobiol. Aging 68, 5–17. https://doi.org/10.1016/j.neurobiolaging.2018.03.025.
Kundra, R., Kornfeld, S., 1999. Asparagine-linked oligosaccharides protect Lamp-1 and Lamp-2 from intracellular proteolysis. J. Biol. Chem. 274, 31039–31046. https://doi.org/10.1074/jbc.274.43.31039.
Lambert, J.C., et al., 2009. Genome-wide association study identifies variants at CLU and CR1 associated with Alzheimer's disease. Nat. Genet. 41, 1094–1099. https://doi.org/10.1038/ng.439.
Letenneur, L., et al., 2008. Seropositivity to herpes simplex virus antibodies and risk of Alzheimer's disease: a population-based cohort study. PloS One 3, e3637. https://doi.org/10.1371/journal.pone.0003637.
Li, J., Pfeffer, S.R., 2016. Lysosomal membrane glycoproteins bind cholesterol and contribute to lysosomal cholesterol export. Elife 5. https://doi.org/10.7554/eLife.21635.
Li Puma, D.D., et al., 2019. Herpes simplex virus type-1 infection impairs adult hippocampal neurogenesis via amyloid-beta protein accumulation. Stem Cell. 37, 1467–1480. https://doi.org/10.1002/stem.3072.
Lin, K.A., et al., 2015. Marked gender differences in progression of mild cognitive impairment over 8 years. Alzheimers Dement (N Y). 1, 103–110. https://doi.org/10.1016/j.trci.2015.07.001.
Lista, P., et al., 2011. On the role of autophagy in human diseases: a gender perspective. J. Cell Mol. Med. 15, 1443–1457. https://doi.org/10.1111/j.1582-4934.2011.01293.x.
Lovheim, H., et al., 2015. Reactivated herpes simplex infection increases the risk of Alzheimer's disease. Alzheimers Dement 11, 593–599. https://doi.org/10.1016/j.jalz.2014.04.522.
Lovheim, H., et al., 2019. Herpes simplex virus, APOEvarepsilon4, and cognitive decline in old age: results from the betula cohort study. J Alzheimers Dis 67, 211–220. https://doi.org/10.3233/JAD-171162.
Marcocci, M.E., et al., 2020. Herpes simplex virus-1 in the brain: the dark side of a sneaky infection. Trends Microbiol. 28, 808–820. https://doi.org/10.1016/j.tim.2020.03.003.
McKhann, G., et al., 1984. Clinical diagnosis of alzheimer's disease: report of the NINCDS-ADRDA work group under the auspices of department of health and human services task force on alzheimer's disease. Neurology 34, 939–944.
Moreno-Grau, S., et al., 2019. Genome-wide association analysis of dementia and its clinical endophenotypes reveal novel loci associated with Alzheimer's disease and three causality networks: the GR@ACE project. Alzheimers Dement 15, 1333–1347. https://doi.org/10.1016/j.jalz.2019.06.4950.
Nixon, R.A., 2017. Amyloid precursor protein and endosomal-lysosomal dysfunction in Alzheimer's disease: inseparable partners in a multifactorial disease. Faseb. J. 31, 2729–2743. https://doi.org/10.1096/fj.201700359.
O'Connell, D., Liang, C., 2016. Autophagy interaction with herpes simplex virus type-1 infection. Autophagy 12, 451–459. https://doi.org/10.1080/15548627.2016.1139262.
Peric, A., Annaert, W., 2015. Early etiology of Alzheimer's disease: tipping the balance toward autophagy or endosomal dysfunction? Acta Neuropathol. 129, 363–381. https://doi.org/10.1007/s00401-014-1379-7.
Porcellini, E., et al., 2010. Alzheimer's disease gene signature says: beware of brain viral infections. Immun. Ageing 7, 16. https://doi.org/10.1186/1742-4933-7-16.
Protto, V., et al., 2020. Multiple herpes simplex virus-1 (HSV-1) reactivations induce protein oxidative damage in mouse brain: novel mechanisms for alzheimer's disease progression. Microorganisms 8. https://doi.org/10.3390/microorganisms8070972.
Qiao, H., et al., 2020. Herpes simplex virus type 1 infection leads to neurodevelopmental disorder-associated neuropathological changes. PLoS Pathog. 16, e1008899 https://doi.org/10.1371/journal.ppat.1008899.
Qin, Q., Li, Y., 2019. Herpesviral infections and antimicrobial protection for Alzheimer's disease: implications for prevention and treatment. J. Med. Virol. 91, 1368–1377. https://doi.org/10.1002/jmv.25481.
Readhead, B., et al., 2018. Multiscale Analysis of independent alzheimer's cohorts finds disruption of molecular, genetic, and clinical networks by human herpesvirus. Neuron 99, 64–82. https://doi.org/10.1016/j.neuron.2018.05.023 e7.
Recuero, M., et al., 2009. A free radical-generating system induces the cholesterol biosynthesis pathway: a role in Alzheimer's disease. Aging Cell 8, 128–139. https://doi.org/10.1111/j.1474-9726.2009.00457.x.
Reddy, P.H., Oliver, D.M., 2019. Amyloid beta and phosphorylated tau-induced defective autophagy and mitophagy in alzheimer's disease. Cells 8. https://doi.org/10.3390/cells8050488.
Rodrigues, J.P.F., et al., 2019. Host cell protein LAMP-2 is the receptor for Trypanosoma cruzi surface molecule gp82 that mediates invasion. Cell Microbiol. 21, e13003 https://doi.org/10.1111/cmi.13003.
Rodriguez-Rodriguez, E., et al., 2010. Epistasis between intracellular cholesterol trafficking-related genes (NPC1 and ABCA1) and Alzheimer's disease risk. J Alzheimers Dis 21, 619–625. https://doi.org/10.3233/JAD-2010-100432.
Rothaug, M., et al., 2015. LAMP-2 deficiency leads to hippocampal dysfunction but normal clearance of neuronal substrates of chaperone-mediated autophagy in a mouse model for Danon disease. Acta Neuropathol Commun 3, 6. https://doi.org/10.1186/s40478-014-0182-y.
Santana, S., et al., 2012a. Herpes simplex virus type I induces an incomplete autophagic response in human neuroblastoma cells. J Alzheimers Dis 30, 815–831. https://doi.org/10.3233/JAD-2012-112000.
Santana, S., et al., 2012b. Herpes simplex virus type I induces the accumulation of intracellular beta-amyloid in autophagic compartments and the inhibition of the non-amyloidogenic pathway in human neuroblastoma cells. Neurobiol. Aging 33. https://doi.org/10.1016/j.neurobiolaging.2010.12.010, 430 e19-33.
Santana, S., et al., 2013. Oxidative stress enhances neurodegeneration markers induced by herpes simplex virus type 1 infection in human neuroblastoma cells. PloS One 8, e75842. https://doi.org/10.1371/journal.pone.0075842.
Schneede, A., et al., 2011. Role for LAMP-2 in endosomal cholesterol transport. J. Cell Mol. Med. 15, 280–295. https://doi.org/10.1111/j.1582-4934.2009.00973.x.
Settembre, C., et al., 2013. Signals from the lysosome: a control centre for cellular clearance and energy metabolism. Nat. Rev. Mol. Cell Biol. 14, 283–296. https://doi.org/10.1038/nrm3565.
Temme, S., et al., 2010. The herpes simplex virus-1 encoded glycoprotein B diverts HLA-DR into the exosome pathway. J. Immunol. 184, 236–243. https://doi.org/10.4049/jimmunol.0902192.
Tzeng, N.S., et al., 2018. Anti-herpetic medications and reduced risk of dementia in patients with herpes simplex virus infections-a nationwide, population-based cohort study in taiwan. Neurotherapeutics 15, 417–429. https://doi.org/10.1007/s13311-018-0611-x.
Ueo, A., et al., 2020. Lysosome-associated membrane proteins support the furin-mediated processing of the Mumps virus fusion protein. J. Virol. 94 https://doi.org/10.1128/JVI.00050-20.
Ushijima, Y., et al., 2009. Herpes simplex virus type 2 tegument protein UL56 relocalizes ubiquitin ligase Nedd4 and has a role in transport and/or release of virions. Virol. J. 6, 168. https://doi.org/10.1186/1743-422X-6-168.
Van Acker, Z.P., et al., 2019. Endo-lysosomal dysregulations and late-onset Alzheimer's disease: impact of genetic risk factors. Mol. Neurodegener. 14, 20. https://doi.org/10.1186/s13024-019-0323-7.
van der Kant, R., et al., 2019. Cholesterol metabolism is a druggable Axis that independently regulates tau and amyloid-beta in iPSC-derived alzheimer's disease neurons. Cell Stem Cell 24. https://doi.org/10.1016/j.stem.2018.12.013, 363-375 e9.
Whyte, L.S., et al., 2017. Endo-lysosomal and autophagic dysfunction: a driving factor in Alzheimer's disease? J. Neurochem. 140, 703–717. https://doi.org/10.1111/jnc.13935.
Wozniak, M.A., et al., 2009. Herpes simplex virus type 1 DNA is located within Alzheimer's disease amyloid plaques. J. Pathol. 217, 131–138. https://doi.org/10.1002/path.2449.

Glossary

LAMP2: lysosome-associated membrane protein 2
HSV-1: herpes simplex virus type 1
Aβ: amyloid-beta peptide;
SNP: single nucleotide polymorphism
HHV-6A: human herpesvirus type 6A

HHV-7: human herpesvirus type 7